Supporting information

Synthesis, crystal structure, DFT studies and optical/electrochemical properties of two novel heteroleptic Copper(I) complexes and applications in DSSC.

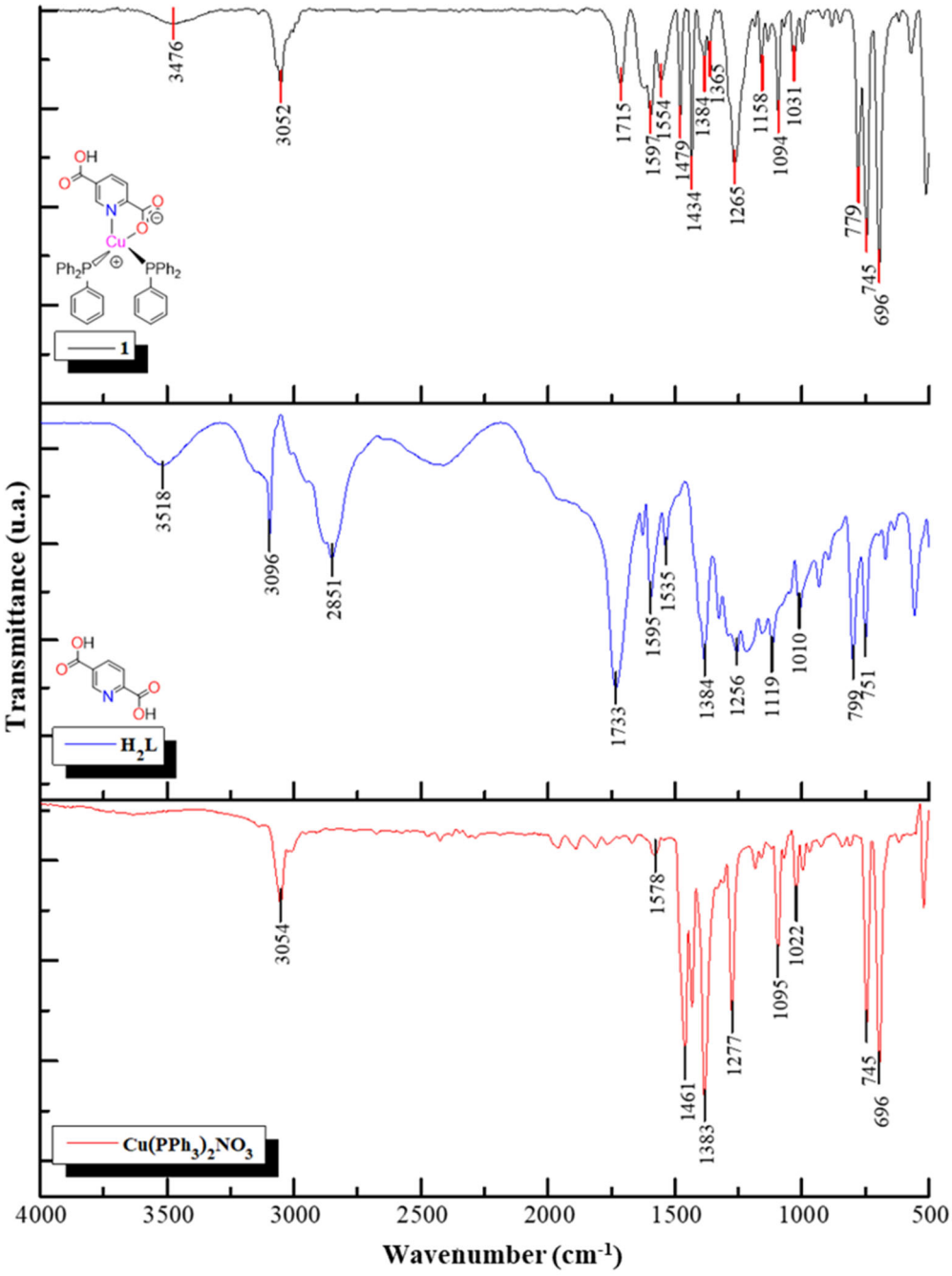

Figure S1. Infrared spectra of complex **1** and the corresponding starting materials.

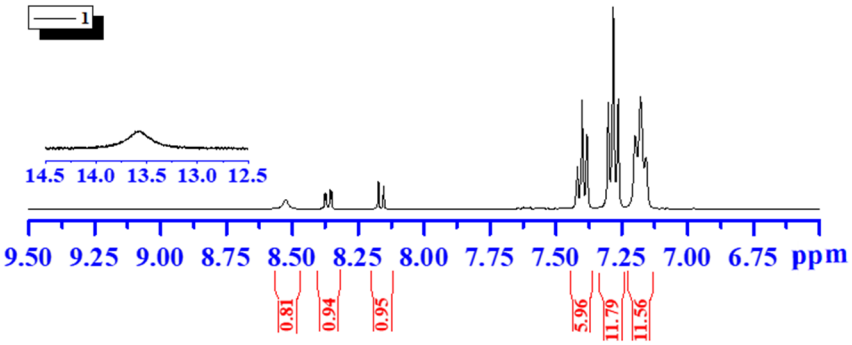

Figure S2. ^{1}H NMR spectrum of **1** in DMSO-d_6.

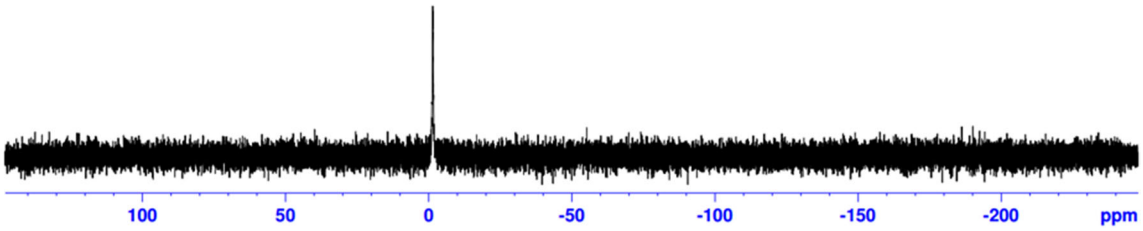

Figure S3. ^{31}P NMR spectrum of **1** in DMSO-d_6.

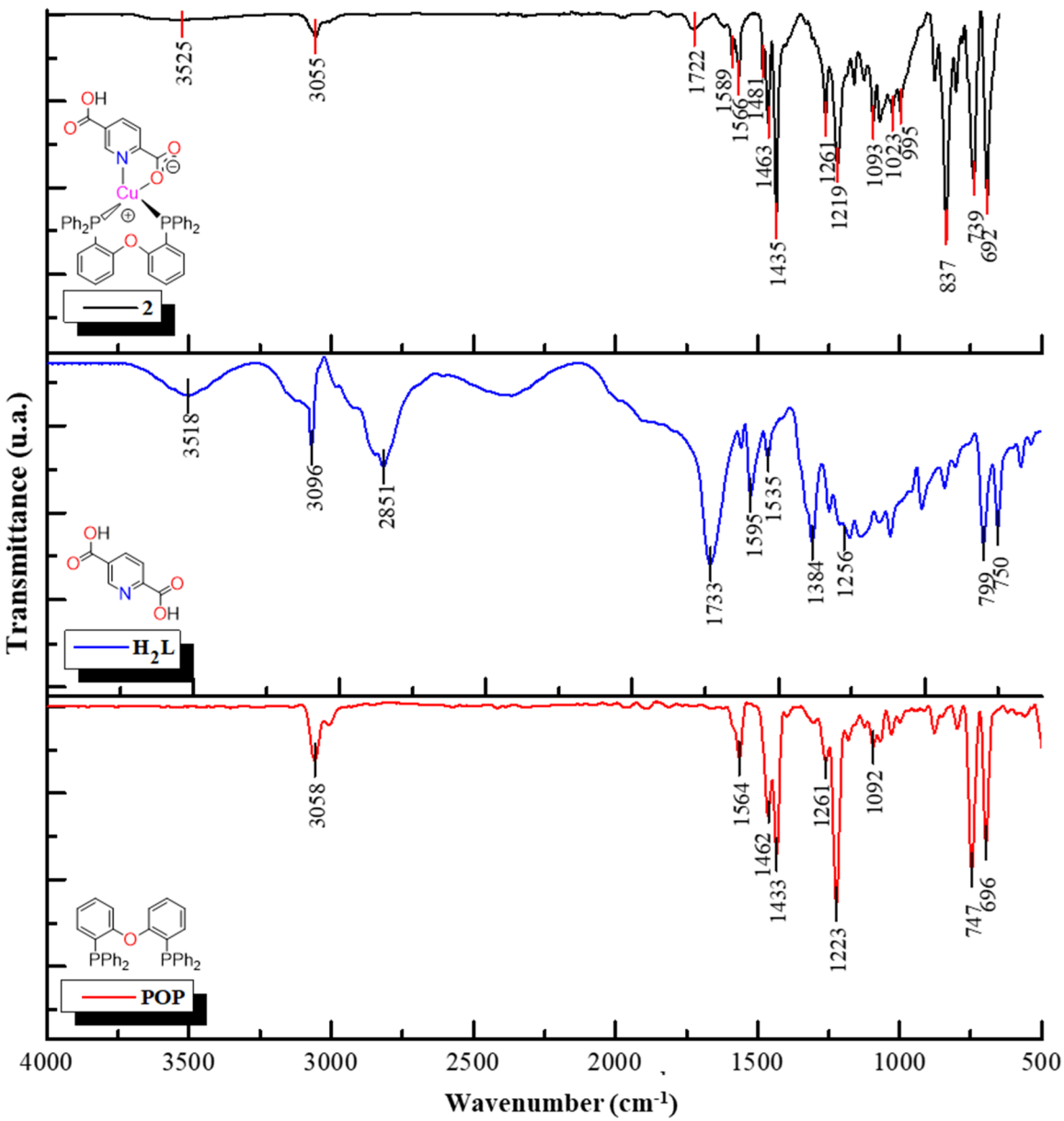

Figure S4. Infrared spectra of complex **2** and the corresponding starting materials.

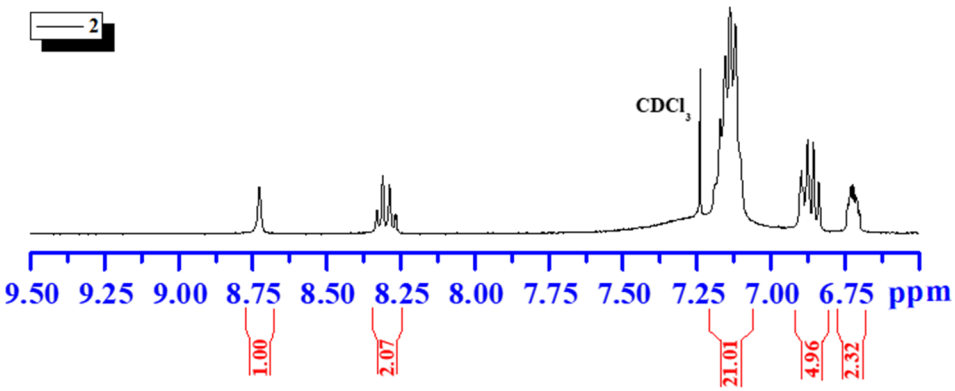

Figure S5. ^{1}H NMR spectrum of **2** in $CDCl_3$.

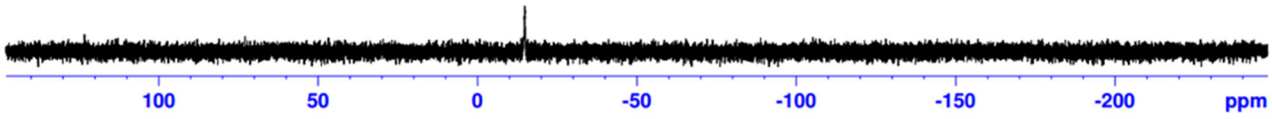

Figure S6. ^{31}P NMR spectrum of **2** in $CDCl_3$

Table S1. Geometries of intermolecular hydrogen bonds and π···π contacts in complexes **1** and **2**.

Complex	*D*−H···*A*	*D*−H [Å]	H···*A* [Å]	*D*···*A* [Å]	∠ *D*−H···*A* [°]	Symmetry code
1	O3−H3···O2	0.82	1.79	2.600(2)	172	x, 1/2−y, −1/2+z
	O31−H31A···O1	0.85	2.63	3.340(2)	143	1−x, −y, 1−z
	O31−H31A···O2	0.85	2.25	3.063(2)	160	1−x, −y, 1−z
	O31−H31B···O4	0.85	2.01	2.857(2)	173	−1+x, y, z
	C3−H3A…O31	0.93	2.57	3.470(3)	163	1+x, y, z
	C16−H16···O31	0.93	2.52	3.355(3)	149	1−x, 1/2+y, 1/2−z
	C17−H17···O4	0.93	2.60	3.489(3)	159	2−x, 1/2+y, 1/2−z
	C34−H34···O1	0.93	2.55	3.361(3)	146	x, 1/2−y, −1/2+z
	C41−H41···O31	0.93	2.49	3.319(3)	149	x, y, z
	C22−H22···Cg1	0.93	3.77	4.404(3)	128	1−x, 1−y, 1−z
	C18−H18···Cg2	0.93	2.72	3.511(3)	143	2−x, 1−y, 1−z
	Cg3···Cg3	–	–	3.739(3)	–	1−x, 1−y, 1−z
2	O5−H5···O2	0.82	1.74	2.555(2)	173	−1/2+x, 1/2−y, 1/2+z
	C6−H6···O4	0.95	2.48	3.255(2)	139	1/2+x, 1/2−y, -1/2+z
	C9−H9···O3	0.95	2.57	3.480(3)	159	−1/2+x, 1/2−y, −1/2+z
	C19−H19···O3	0.95	2.45	3.371(2)	163	1/2−x, 1/2+y, 1/2−z
	C30−H30···O4	0.95	2.49	3.406(3)	162	1/2+x, 1/2−y, −1/2+z
	C44−H44B···O4	0.99	2.33	3.302(3)	166	x, y, z
	C17−H17···Cl1	0.95	2.93	3.506(2)	120	1/2−x, 1/2+y, 1/2−z
	C42−H42···Cl1	0.95	2.89	3.752(2)	152	x, y, z
	C15−H15···Cg4	0.95	3.17	4.003(4)	148	−1/2+x, 1/2−y, −1/2+z
	C23-H23···Cl2	0.95	2.98	3.415(2)	110	1/2−x, 1/2+y, 3/2−z

1: Cg1 = N1, C1, C2, C3, C4, C5; Cg2 = C8, C9, C10, C11, C12, C13; Cg3 = C20, C21, C22, C23, C24, C25. **2**: Cg4 = C1, C2, C21, C22, C23, C24.

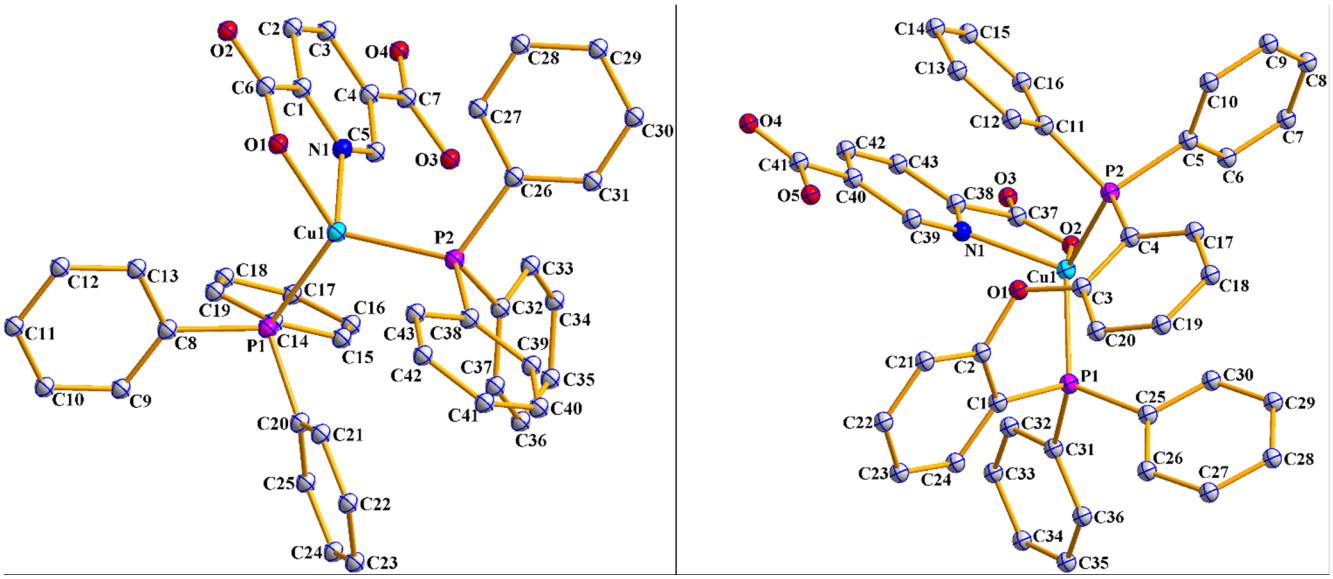

Figure S7. Geometry-optimized structures of complexes **1** (left) and **2** (right) at the M06/6-31G(d)+DZVP level of theory. Hydrogen atoms are omitted for clarity.

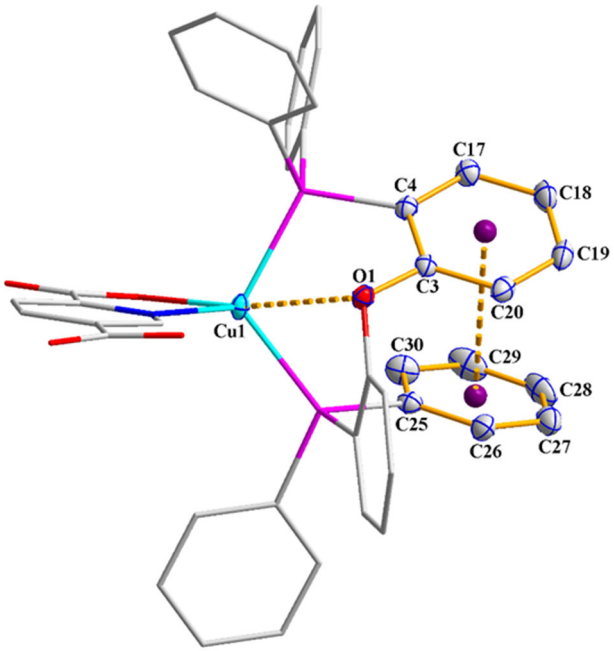

Figure S8. Intramolecular Cu1···O1 and π···π interactions in the crystal structure of **2**. Hydrogen atoms have been omitted for clarity.

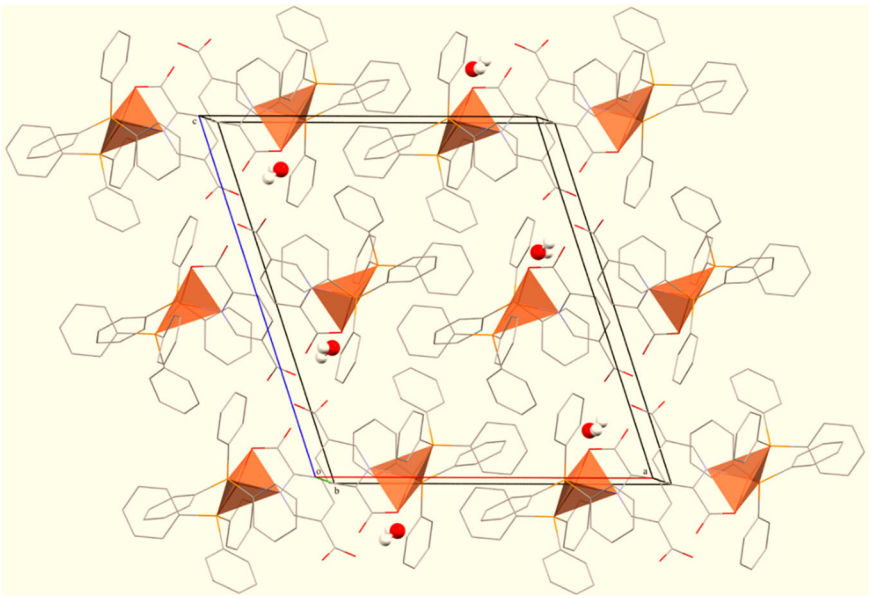

Figure S9. Perspective view of the three-dimensional (3D) hydrogen-bonded network in the crystal structure of complex **1**, formed through O-H···O^-, O_w-H···O^-, O_w-H···$O_{c=o}$, C-H···O^-/O_w/$O_{c=o}$, C-H···π and π···π interactions. Hydrogen atoms have been omitted for clarity.

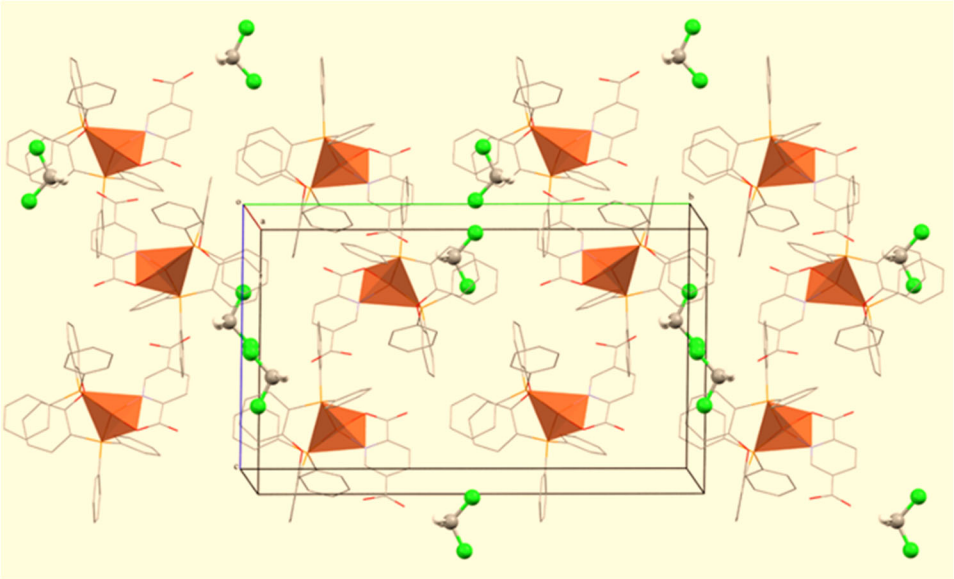

Figure S10. Perspective view of the three-dimensional (3D) hydrogen-bonded network in the crystal structure of complex **2**, formed through O-H···O^-, C-H···O^-/$O_{c=o}$, C-H···Cl, C-Cl···π and C-H··· π interactions. Hydrogen atoms are omitted for clarity.

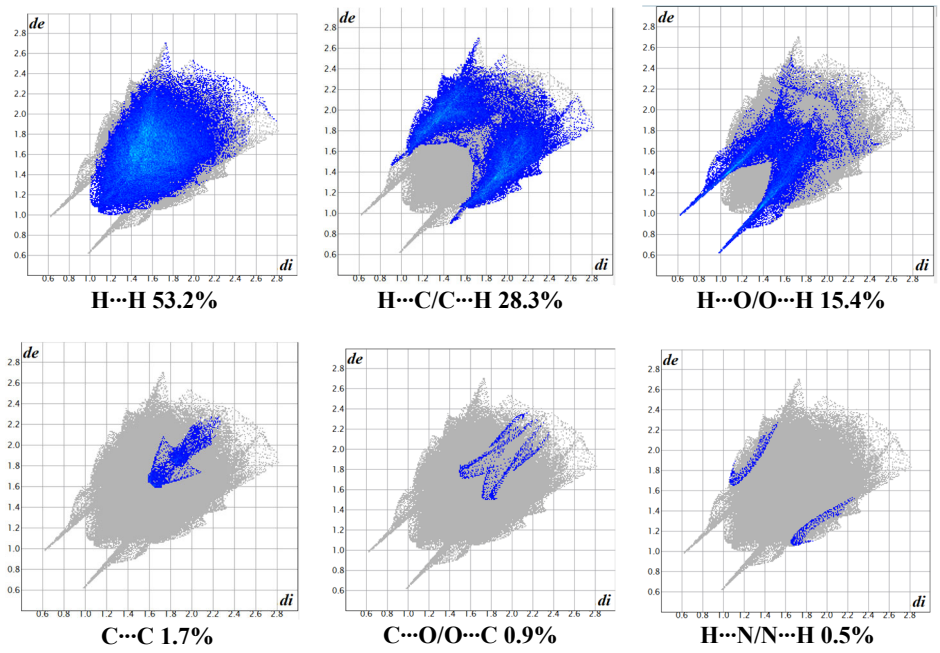

Figure S11. Percentages of intermolecular interactions in the fingerprint plot for complex **1**

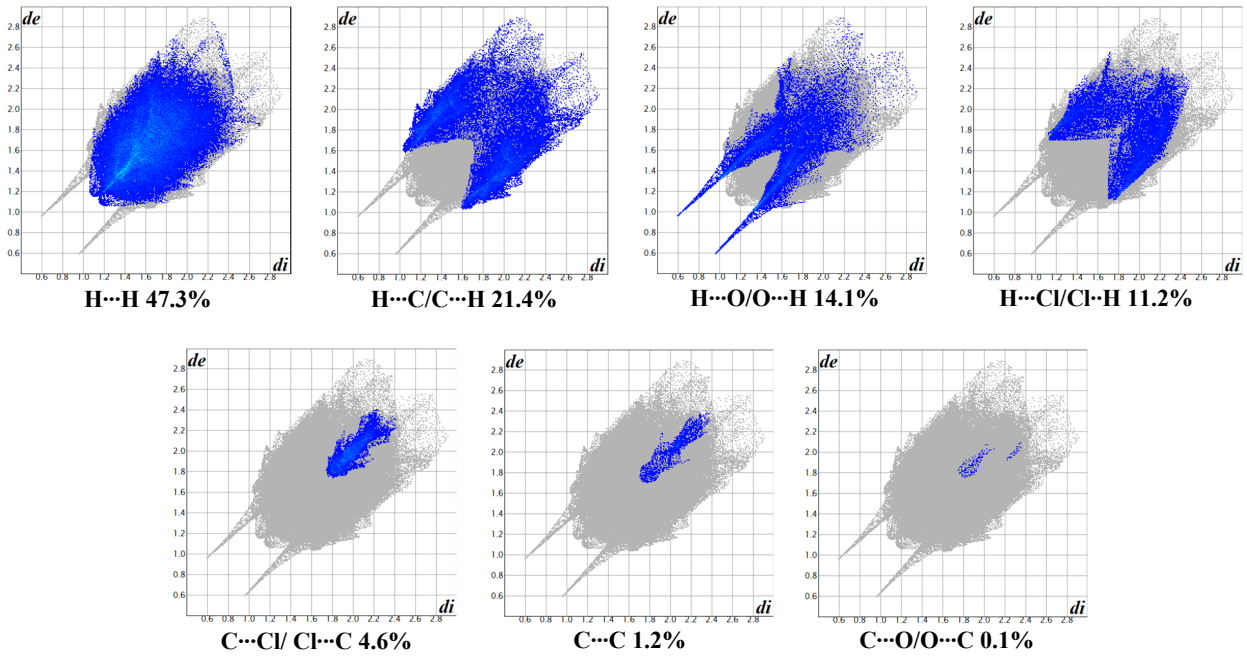

Figure S12. Percentages of intermolecular interactions in the fingerprint plot for complex **2**

Molecular Orbitals
*Complex **1***
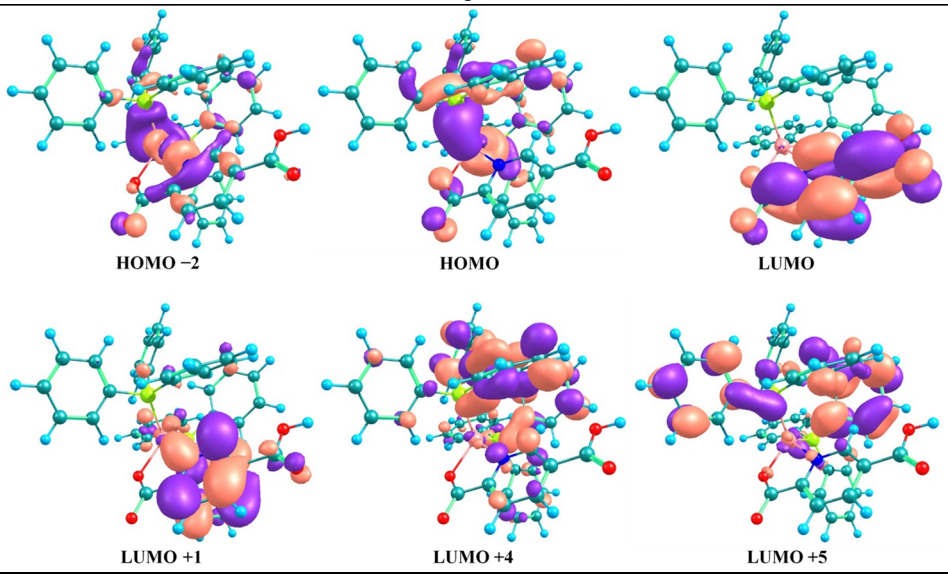
*Complex **2***
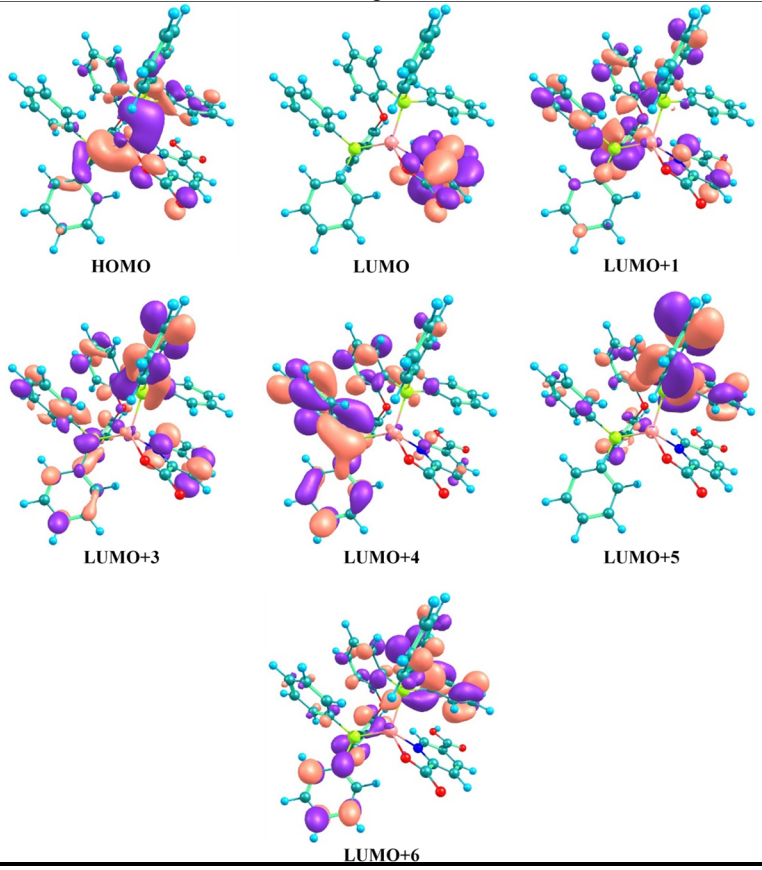

Figure S13. HOMO and LUMO frontier orbital plots of complexes **1** and **2** based on TD-DFT calculations.

Table S2. Data extracted from the calculated electronic absorption spectra using Time-dependent Density Functional Theory (TD-DFT) at the level M06-2X/6-31G(d)+DZVP for complexes **1** and **2**.

Complex	λ_{DFT} (nm)	λ_{Exp} (nm)	Character	Transitions (CI Coef.)	*f*	HOMO (eV)	LUMO (eV)	ΔE (eV)
1	421	364	$MLCT_{Cu\rightarrow L}/LLCT_{(PPh_3)_2\rightarrow L}$	HOMO→LUMO (99%)	0.0145	−5.918	−1.825	4.093
	328	265	$MLCT_{Cu\rightarrow L/(PPh_3)_2}/LLCT_{(PPh_3)_2\rightarrow L}/\pi\rightarrow\pi^*_{(PPh_3)_2\rightarrow(PPh_3)_2}$	HOMO→LUMO+1 (98%)	0.0367	−5.918	−0.949	4.969
	287	265	$MLCT_{Cu\rightarrow L/(PPh_3)_2}/LLCT_{(PPh_3)_2\rightarrow L}/\pi\rightarrow\pi^*_{(PPh_3)_2\rightarrow(PPh_3)_2}$	HOMO→LUMO+4 (92%)	0.0406	−5.918	−0.673	5.245
	279	265	$MLCT_{Cu\rightarrow L/(PPh_3)_2}/LLCT_{(PPh_3)_2\rightarrow L}/\pi\rightarrow\pi^*_{(PPh_3)_2\rightarrow(PPh_3)_2}$	HOMO→LUMO+5 (85%)	0.0266	−5.918	−0.551	5.367
2	422	383	$MLCT_{Cu\rightarrow L}/LLCT_{POP\rightarrow L}$	HOMO→LUMO (99%)	0.0136	−5.857	−1.775	4.082
	327	265	$MLCT_{Cu\rightarrow POP/L}/LLCT_{POP\rightarrow L}/\pi\rightarrow\pi^*_{POP\rightarrow POP}$	HOMO→LUMO+1 (97%)	0.0376	−5.857	−0.956	4.901
	302	265	$MLCT_{Cu\rightarrow POP/L}/LLCT_{POP\rightarrow L}/\pi\rightarrow\pi^*_{POP\rightarrow POP}$	HOMO→LUMO+3 (86%)	0.0484	−5.857	−0.829	5.028
	293	265	$MLCT_{Cu\rightarrow POP/L}/LLCT_{POP\rightarrow L}/\pi\rightarrow\pi^*_{POP\rightarrow POP}$	HOMO→LUMO+4 (93%)	0.0411	−5.857	−0.801	5.056
	282	265	$MLCT_{Cu\rightarrow POP}/\pi\rightarrow\pi^*_{POP\rightarrow POP}$	HOMO→LUMO+5 (90%)	0.0521	−5.857	−0.632	5.225
	273	265	$MLCT_{Cu\rightarrow POP}/\pi\rightarrow\pi^*_{POP\rightarrow POP}$	HOMO→LUMO+6 (66%)	0.0407	−5.857	−0.433	5.424

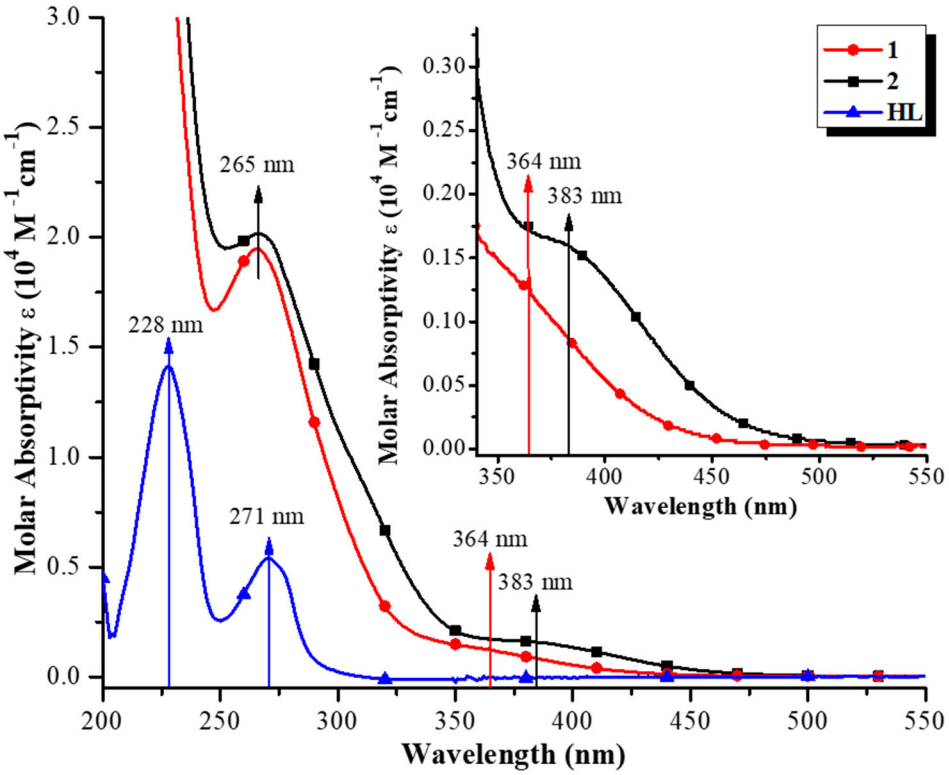

Figure S14. UV-vis absorption spectra of **1**, **2** and free ligand **H_2L** recorded for a 6x10^{-5}mol/L solution in EtOH**.**

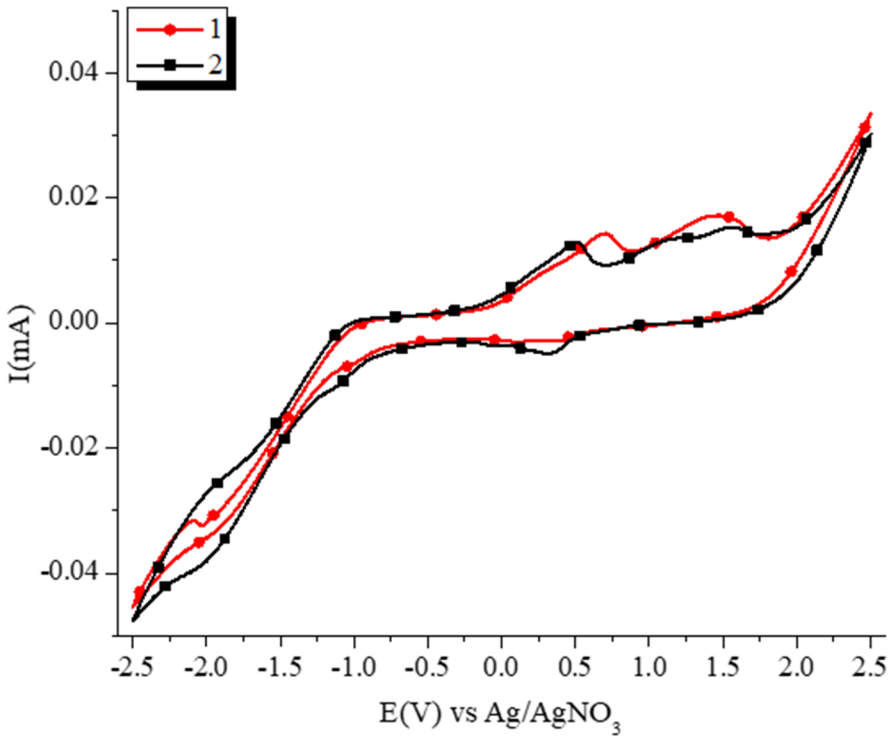

Figure S15. Cyclic voltammograms of **1** and **2** (ca. $8x10^{-5}$ M) in EtOH and CH_2Cl_2, respectively, at $T = 298$ K using $(nBu_4N)PF_6$ (0.025 M) as supporting electrolyte (scan rate = 100 mVs^{-1}).